sustainability

MDPI

Article

Heavy Metal Content and Pollution Assessment in Typical Check Dam Sediment in a Watershed of Loess Plateau, China

Yongxia Meng, Peng Li *, Lie Xiao, Rui Wang, Shutong Yang, Jiangxue Han and Bingze Hu

State Key Laboratory of Eco-Hydraulics in Northwest Arid Region of China, Xi'an University of Technology, Xi'an 710048, China; myxia94@163.com (Y.M.); xiaosha525@163.com (L.X.); wr92333@163.com (R.W.); ystong@163.com (S.Y.); hanjiangxue0118@163.co (J.H.); 18832017493@163.com (B.H.)
* Correspondence: lipeng74@163.com

Abstract: To understand historical trends and assess the ecological risk associated with heavy metal pollution, the concentration of eight species of heavy metals (vanadium (V), chromium (Cr), manganese (Mn), cobalt (Co), nickel (Ni), zinc (Zn), copper (Cu), and arsenic (As)) in typical silt dam sediments on the Loess Plateau were analyzed. The radionuclide ^{137}Cs was used to quantify rates of erosion, deposition, and heavy metal contamination in the soils of a watershed that supplies a check dam. The sediment record revealed three time periods distinguished by trends in erosion and pollutant accumulation (1960–1967, 1968–1981, and 1985–1991). Heavy metal concentrations were highest but exhibited significant fluctuation in the first two periods (1960–1967 and 1968–1981). From 1985 to 1991, heavy metal pollution showed a downward trend and tended to be stable. The potential risks of heavy metals in silt dam sediments were explored by applying the geo-accumulation index and the potential ecological risk index. The results indicated medium risk associated with Cu and As accumulation, especially in 1963, 1971, and 1986 when the assessed values increased significantly from previous levels. Agricultural practices and high rates of slope erosion may be responsible for the enrichment of As and Cu in soil and the accompanying increase in risk. Land use optimization and the careful use of fertilizers could be used to control or intercept heavy metal pollutants in dammed lands. The results provide the basis for evaluating the current status and ecological risk of heavy metal contamination in dam sediments and for predicting possible heavy metal pollution in the future.

Keywords: check dam; ecological risk assessment; Loess Plateau; soil heavy metal

Citation: Meng, Y.; Li, P.; Xiao, L.; Wang, R.; Yang, S.; Han, J.; Hu, B. Heavy Metal Content and Pollution Assessment in Typical Check Dam Sediment in a Watershed of Loess Plateau, China. *Sustainability* **2022**, *14*, 8597. https://doi.org/10.3390/su14148597

Academic Editor: Iain J. Gordon

Received: 6 June 2022
Accepted: 11 July 2022
Published: 14 July 2022

1. Introduction

Rapid industrial and agricultural expansion has resulted in widespread heavy metal contamination in soils. Because heavy metals are persistent and toxic, and in some cases, irreversibly bound to soil minerals or soil organic matter, this type of pollution presents serious risks to human health and economic development. [1,2]. Heavy metals can originate from natural sources (e.g., rock weathering, soil parent material, etc.) or from artificial sources (e.g., industrial and agricultural production, traffic pollution, etc.) and can accumulate over time [3]. When agricultural production takes place on soils enriched in heavy metals, these toxic substances infiltrate the food chain, creating substantial risks to human health [4–7].

On the Loess Plateau in Northwest China, heavy rainfall coupled with intense human activity has resulted in heavy erosion [8–11]. Starting in the 1950s, the government began implementing engineering and forestry measures intended to conserve water and reduce rates of erosion [12]. As part of this strategy, an extensive network of warping dams was constructed across the Plateau. These dams block sediment export by retaining and depositing soil materials dislodged by erosive rainfall. Not only do warping dams reduce soil loss from erosion, but the resulting alluvial deposits enhance the Plateau's fertility [13,14].

The sediment retained by warping dams integrates information about natural and anthropogenic processes occurring in the area (e.g., pollution of As and Cu in cultivated soil). Because soils are a major sink for heavy metals, the sediment contains a record of pollution in the area. Moreover, when environmental conditions (e.g., temperature, pH, and organic matter content) change, heavy metals may be redistributed in the sediment, causing secondary contamination [15,16]. Thus, establishing the sequence of sedimentary ages can reveal the historical inputs and associated trends in heavy metal pollution.

Soil pollution is typically evaluated using the geo-accumulation index (I_{geo}) in conjunction with the potential ecological risk coefficient (E_r^i) [17,18]. This method has been used by researchers to study, for example, Cadmium contamination in near-shore sediments of the Yellow River [17] and heavy metal contamination in surface sediments of the Bay of Bengal estuary [18]. Recently, scientists have begun augmenting these methods with GIS geostatistical analysis and artificial neural network models to produce maps depicting the spatial distribution of pollutants [19].

Heavy metal pollution in river sediment has been widely studied [20–23]. However, there are few studies describing how the distribution and chemistry of heavy metals changes over time in check dam sediments. In this study, the age and deposition rate of heavy metals were determined using the radionuclide cesium-137 (^{137}Cs). The heavy metal content of stratified samples was also assessed to derive age-specific heavy metal accumulation characteristics. Together, this information provides the basis for evaluating the current status of dam site sediments and predicting possible future heavy metal contamination. The objectives of this study were: (1) to identify the age of check dam sediments; (2) to identify how the heavy metal content in check dam sediment varies over time; and (3) to evaluate the extent of heavy metal pollution in dam land.

2. Materials and Methods

2.1. Study Sites

The 5.97 km^2 Wangmaogou watershed is situated in the Loess Plateau (110°20′49.5″ E–110°21′00.3″ E, 37°35′36.3″–37°35′11.2″ N) at an altitude of 940–1188 m, with an annual average erosion modulus of 18,000 t/km^2·a [24]. The Nianyangou watershed is a small branch of the Wangmaogou watershed, with an elevation between 1027 and 1188 m. The Nianyangou watershed has three silt dams, of which two have drainage structures while the third has no water release structure. This study focused on the basin of the third Nianyangou dam located within the first branch of the Wangmaogou watershed. Built in 1956 and silted in 1990, this dam has controlled an area of 0.46 km^2 for 34 years. As rainfall scours the area, the dam intercepts sediments formed when topsoil on the slope of the basin is dislodged from areas of different land use types (e.g., slope farmland, shrubland, and grassland).

2.2. Sampling and Testing

Samples were collected from Nianyan Ditch in Suide County on 25 July 2020 (Figure 1). Three gravity samplers (10 cm in diameter) were used to collect columnar sediment samples along the dam at a depth of 6.5 m. After collection, complete sediment samples were divided into cyclic layers if boundaries were easily distinguishable based on color and particle composition. Each of the 77 columnar samples collected was divided into 29 layers and placed in a clean plastic bag for immediate shipment to the laboratory for cryogenic (4 °C) storage. After samples were air-dried, impurities were removed and they were passed through a 0.155 mm (100 mesh) sieve in preparation for testing.

Each sample was evenly mixed and 0.10 g (accurate to 0.0001 g) subsamples were placed in an X-press digestion tube. Aqua regia (nitrohydrochloric acid) was prepared by mixing concentrated hydrochloric acid (HCl) and concentrated nitric acid (HNO_3) in a 3:1 ratio by volume. Microwave digestion was performed using the following procedure: A total of 6 mL aqua regia was added to each X-press tube containing a sample, after which the tube was placed in a microwave digestion instrument. The sample was heated to 120 °C

over an interval of 5 min and held at the target temperature for 2 min. The temperature was increased again over a period of 8 min to 185 °C, where it was held for 40 min. Samples were allowed to cool to room temperature, after which they were placed in a fume hood. Acid was driven off by heating the digested samples to 120 °C and holding for 2 min. The solution was passed through filter paper into a 50 mL volumetric flask, after which the digestion tube and filter paper were cleaned 3 times with 5% dilute nitric acid. The final volume was fixed using deionized water.

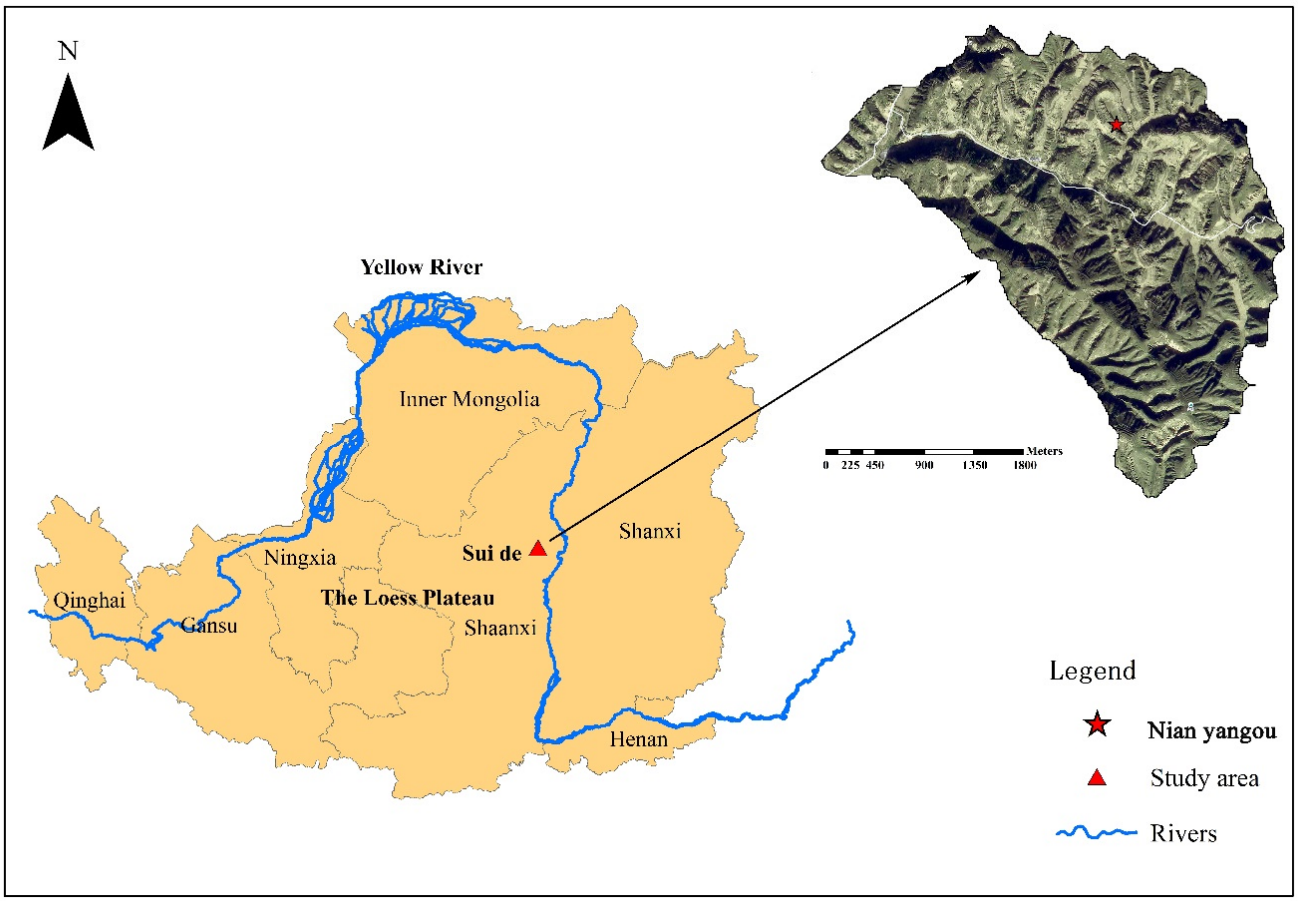

Figure 1. Map of the study area.

An inductively coupled plasma mass spectrometer (ICP-MS, Agilent Technologies, Santa Clara, CA, USA) was used to determine the concentration of the eight heavy metals of interest (V, Cr, Mn, Co, Ni, Cu, Zn, and As). To ensure analytical precision, relative standard deviation (RSD) values were calculated for instrument sensitivity, oxides, double charge parameters, and the signal intensity of elements in the tuning solution. Experimental results with RSD values >5% for any factor were rejected. Before running a blank measurement, the system was flushed with 5% nitric acid until the analytical signal was stabilized. The recoveries of soil samples ranged from 87.8% to 111.0%.

Soil ^{137}Cs was measured by a high purity germanium γ spectrometer (ORTEC, Oak Ridge, TN, USA) analyzer. The determination time for each sample was 28,800 s. The mass activity of ^{137}Cs was calculated from the net area of 661.62 KeV rays, and the relative error of samples was less than 10%. Soil bulk density was determined for each divided cyclic layer by collecting the undisturbed 200 cm^3 soil core using a ring knife. The sample was weighed, dried in an oven at 105 °C for 16 h, then reweighed after cooling to 25 °C.

2.3. Data Analysis

2.3.1. Calculation of Soil Bulk Density

Soil bulk density was calculated using [25]:

$$\rho_b = G \times 100/(v \times (100 + w)) \quad (1)$$

where ρ_b is the soil bulk density (g/cm^3), G is weight of the field moist soil sample (g), v is the internal volume of the ring knife (cm^3), and w is the soil moisture content.

2.3.2. Calculation of Cyclic Layer Sediment Weight and Total Sediment Weight

Cyclic layer sediment and total sediment volume were calculated using the formulas from [26]:

$$M_i = V_i \times \rho_i \; i = 1, 2, \ldots \mathrm{n} \quad (2)$$

$$M = \sum_1^n M_i \quad (3)$$

where V_i is the volume of the i-th sedimentary cycle (m^3); ρ_i is the unit weight of the i-th sedimentary cycle (g·cm^{-3}); M_i is the sediment deposition volume of the i-th sediment cycle (t); M is the gross amount of sediment retained (t).

2.3.3. Calculation of Heavy Metal Deposition Rate

Heavy metal deposition rate was calculated using [26]:

$$W = \Delta M/(T_2 - T_1) \quad (4)$$

$$\Delta M = \sum B_i \times h_i \quad (5)$$

$$\sum h_i = \Delta H \quad (6)$$

where T_1 and T_2 are the start and end years of the period estimated using ^{137}Cs, respectively; ΔH is the thickness corresponding to the interval between T_1 and T_2; ΔM is the mass of sediment per unit area (g/cm^2) corresponding to ΔH; B_i and h_i are the deposit bulk density (g/cm^3) and thickness (cm), respectively; and W is the deposition rate of heavy metals (g/cm^2·a).

2.3.4. Risk Analysis

The geo-accumulation index (I_{geo}), also known as the Muller index, is an important parameter used to distinguish the impact of human activities [27]. It is calculated using the equation:

$$I_{geo} = log_2[C_n/(1.5B_n)] \quad (7)$$

where I_{geo} is the geo-accumulation index, C_n is the measured concentration of heavy metals in soil, B_n is the geochemical background concentration of soil heavy metals, and 1.5 is the background matrix correction factor.

The potential risk index (E_r^i) considers the types, contents, and toxicity levels of pollutants in sediments to quantify ecological risk [28]. It was calculated using the equation:

$$C_i^f = \frac{C_s^i}{C_n^i} \quad (8)$$

$$E_r^i = T_r^i \times C_f^i \quad (9)$$

$$RI = \sum_{i=1}^n E_r^i \quad (10)$$

where C_i^f is the pollution coefficient of a metal, C_s^i the measured value of heavy metals, C_n^i is the parameter ratio, E_r^i is the potential ecological risk coefficient of heavy metals , T_r^i is the response coefficient of metal toxicity, and RI is the comprehensive potential ecological damage index of various heavy metals.

Evaluations of risk using this metric vary depending on the background knowledge of the person using it. Because of its subjective nature, the potential risk index is notoriously difficult to use. The types of heavy metal elements measured in this paper are different from the eight elements evaluated by Hakanson (1980). Therefore, the Hakanson criteria cannot be used to evaluate heavy metal pollution in sediments collected in the Nianyan Ditch [29]. E_r^i for these samples was calculated using T_r^i values determined by Xu et al. (2008) (Table 1) [30].

Table 1. Response coefficient values of heavy metals in dam sediments.

Element	V	Cr	Mn	Co	Ni	Cu	Zn	As
Toxicity Coefficient	2	2	1	5	5	5	1	10

To fit the area assessed in Nianyan Ditch, the ecological hazard index for heavy metals in the study area was adjusted using the risk intensity limit adjustment method developed by Lin et al. (Table 2) [31].

Table 2. Ecological risk index and risk intensity grade associated with Nianyan Ditch sediments.

E_r^i	Degree	*RI*	Degree
<9	Slight	<35	Slight
$9 \leq r < 18$	Medium	$35 \leq RI < 70$	Medium
$18 \leq r < 37$	Considerable	$70 \leq RI < 140$	Considerable
$37 \leq r < 75$	Very strong	$RI \geq 140$	Very strong
$75 \leq r$	Extremely strong		

Note: E_r^i is the potential ecological risk coefficient of heavy metals; *RI* is the comprehensive potential ecological damage index.

3. Results

3.1. Determination of Sediment Age

During a typical rainstorm, eroded materials are transported along the runoff path and deposited in front of the dam, forming a layer of sediment. Each of these layers is formed by a single depositional event, resulting in the development of a stratified sedimentary bed [32]. The date at which each cyclic layer formed can be determined using weather records, sediment volume, and ^{137}Cs activity.

The mass specific activity of ^{137}Cs in the samples collected for this study varies with depth (Figure 2). Two storage peaks are obvious: the main storage peak (4.86 Bq/kg) at a depth of 530 cm and the second storage peak (3.99 Bq/kg) at a depth of 154.8 cm. Globally, the abundance of ^{137}Cs peaked in 1963 as the result of nuclear weapons testing [33] and crested again in 1986 following the Chernobyl nuclear leakage event [34]. Based on the depth profile of ^{137}Cs activity, it was determined that the deep storage peak (layer 24) formed in 1963 and the shallow storage peak (layer 7) formed in 1986. Cyclic layers containing greater sedimentary volume correspond to heavy, erosive rainfall events, which allowed for the development of the more highly resolved timeline presented in Figure 2.

3.2. Patterns of Heavy Metal Concentration in the Dam Sediment Site over Time

The soil profile distribution of heavy metals in the sediment reflects the depositional record of each element, and the change in each stage reflects different geochemical behaviors. Concentrations of heavy metals in the soil profile at Nianyangou are greatly varied. The contents of V, Cr, Mn, Co, Ni, As, Zn, and Cu are 32.83–75.04, 30.36–122.54, 440.06–774.69, 12.60–28.35, 19.26–44.56, 17.99–51.34, 56.23–130.44, and 10.97–22.08, respectively. The sampled sediments are relatively enriched in Zn and Mn, mostly due to their high abundance in the crust. The variation of each heavy metal with depth is shown in Figure 3, and the direction of change in concentration (i.e., increasing or decreasing) is roughly mirrored across all eight metals at a given depth.

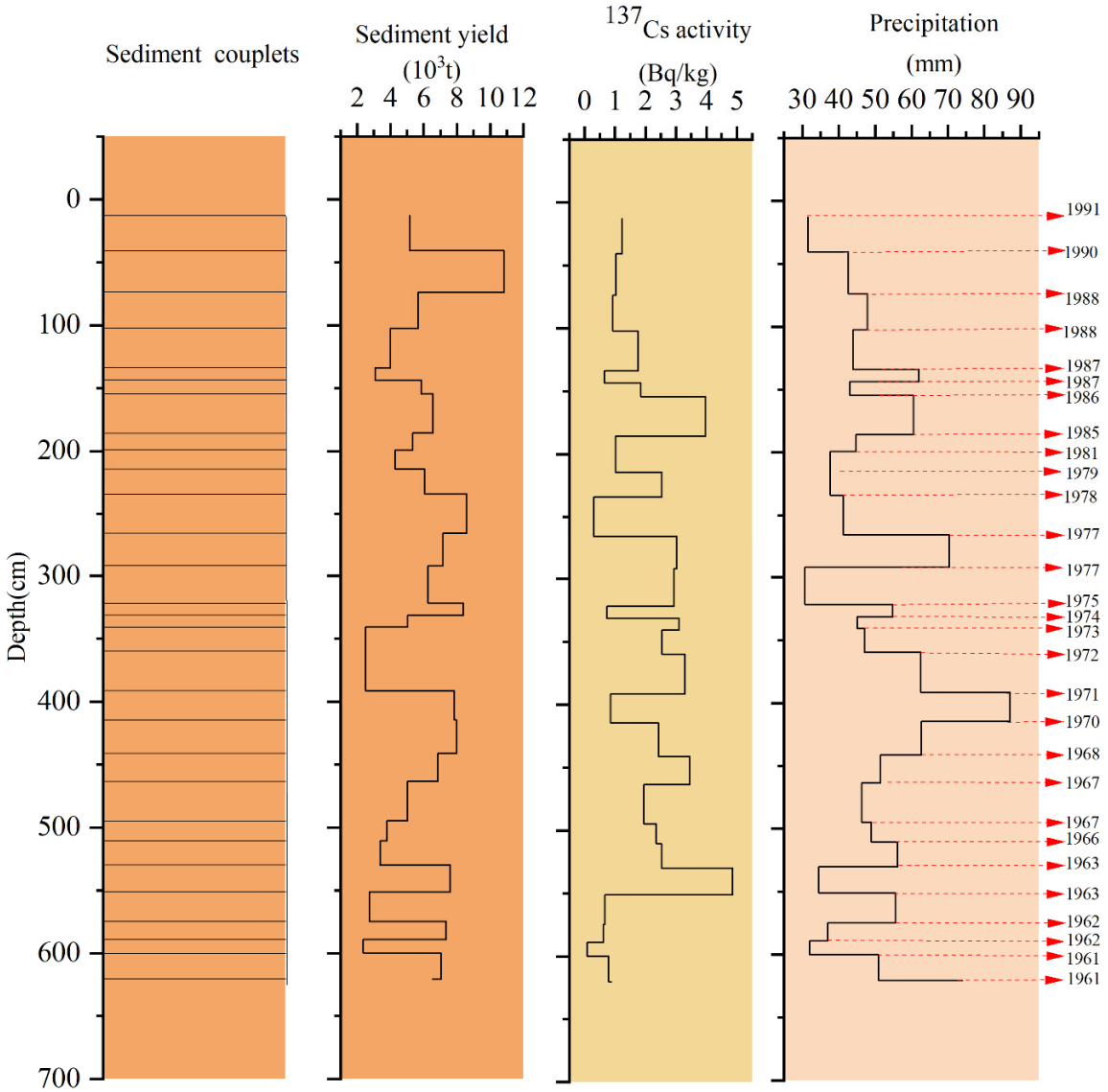

Figure 2. Cyclic layer thickness, ^{137}Cs activity, and precipitation data for sampled sediment.

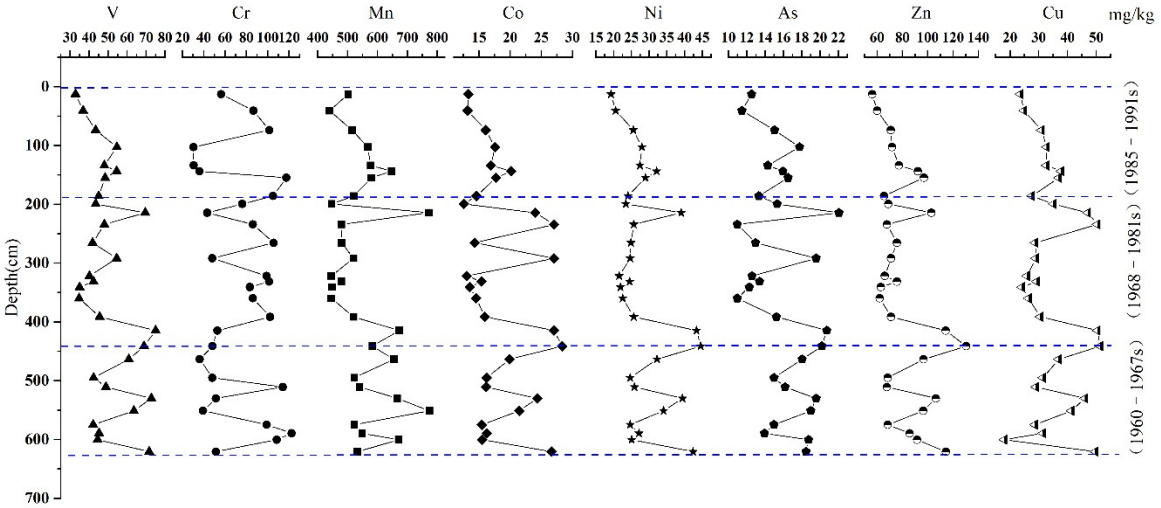

Figure 3. Distribution of heavy metals with depth in dam sediment.

Based on ^{137}Cs activity, thickness of the silt layer, and the vertical distribution of heavy metals, the sediment core was divided into three distinct time periods. The deepest core segment corresponds to the period between 1960 and 1967. This section is distinctive because of its thick silt layer, reflecting the strong erosion of the drainage basin and high rates of sediment deposition during this period. This segment is also notable because a decrease in Cr concentration in 1963 was coupled with large increases in the concentration of each of the seven other heavy metals. The middle segment corresponds to a period spanning from 1968 to 1981. Though there were a few thick layers in this section, cyclic layers are generally thin, indicating reduced rates of erosion. The concentration of heavy metals in this segment greatly fluctuated: the concentration of Cr increased and then decreased, while the concentrations of V, Mn, Co, Ni, As, Zn, and Cu demonstrate an opposite trend, decreasing first before increasing. The shallowest segment corresponds to a period from 1985 to 1991. This section is notable because the thickness of the silt layer increased, indicating higher rates of erosion. However, the content of heavy metals in this stage tended to be stable, with generally lower rates of pollution compared to the previous two periods.

3.3. Assessment of Heavy Metal Pollution

Overall, values of I_{geo} in sampled sediment were between −1.62 to 0.83 (Figure 4), indicating slight to no pollution. Values of I_{geo} for Cr, Co, Cu, Zn, and As indicate slight contamination, with pollution proportions of 37.93%, 64.29%, 75%, 32.14%, and 32.14%, respectively.

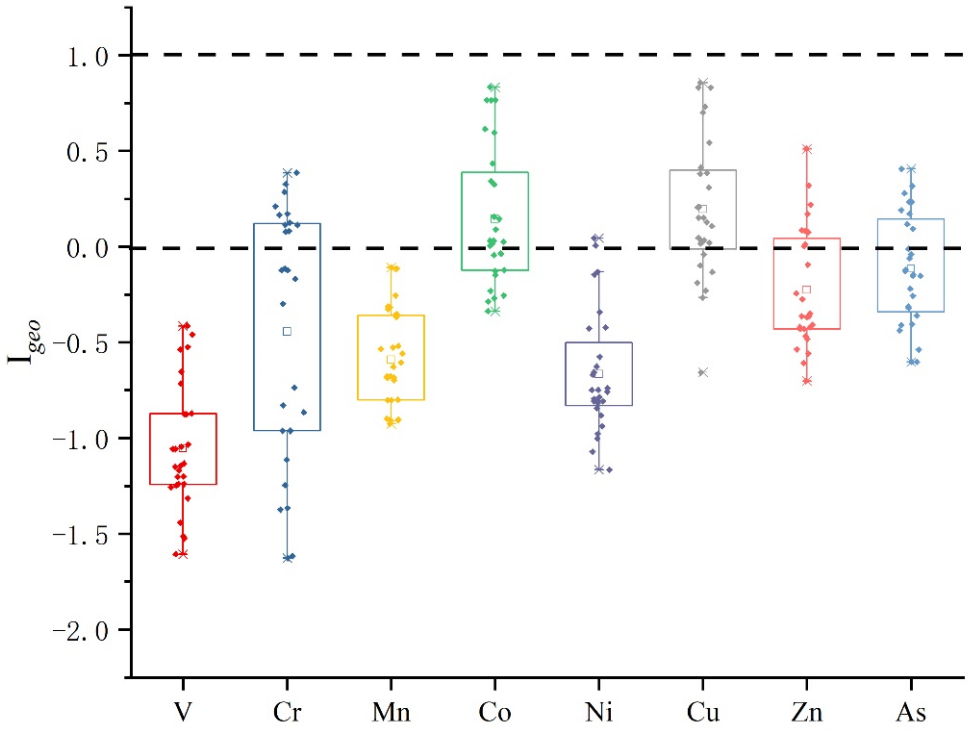

Figure 4. Geo-accumulation index (I_{geo}) values of heavy metals in dam sediment.

In the first time period, heavy metal contamination reached its peak in 1963, with I_{geo} values in the slight pollution range: 0.52, 0.24, and 0.62 for Co, Cu, and As, respectively. The second time period was also marked by slight pollution, which peaked in 1971 with I_{geo} values of 0.83, 0.86, 0.51, and 0.28 for Co, Cu, Zn, and As, respectively. In the third period, heavy metal pollution was at its lowest, with only two heavy metals having I_{geo} values indicating light pollution: 0.38 and 0.32 for Cu and Cr, respectively.

The potential risk index values (E_r^i) were ranked from from highest to lowest: As > Cu > Co > Ni > Cr > V > Zn > Mn. Among them, the risk degree of V, Cr, Mn, Ni, and Zn was low, and their E_r^i values were less than nine. The E_r^i values of Co and

Cu ranged from 5.94 to 15.09 and 4.76 to 13.58, respectively. For Co and Cu, 65.52% and 62.10% of the sampling points showed low risk, respectively, and 34.40% and 37.90% of the sampling points showed medium risk. The values of As ranged from 9.86 to 18.69, and 89.60% of the sampling points were at medium risk (Table 3). The E_r^i values of the three heavy metals Co, Cu, and As increased significantly in 1963, 1971, and 1986 to values indicating moderate risk, which was consistent I_{geo} values for those years. The RI of the eight heavy metals ranged from 31.78 to 59.69, and 78.56% of the sampling points were at medium risk. The average contributions of As and Cu to the RI were 32.9% and 20.9%, respectively, while the average contribution rate of the remaining eight heavy metals to the RI was 46.20% (Figure 5). Although concentrations of As and Cu in the dam sediments were low, their potential ecological risks were high.

Table 3. Contribution of each heavy metal to ecological risk assessment values.

E_r^i	Proportion(%)								RI	Proportion (%)
	V	Cr	Mn	Co	Ni	Cu	Zn	As		
Slight	100	100	100	65.52	100	62.1	100	10	Slight	24.14
medium	0	0	0	34.48	0	37.93	0	89.65	medium	75.86
Considerable	0	0	0	0	0	0	0	0	Considerable	0
Very strong	0	0	0	0	0	0	0	0	Very strong	0
Extremely strong	0	0	0	0	0	0	0	0		

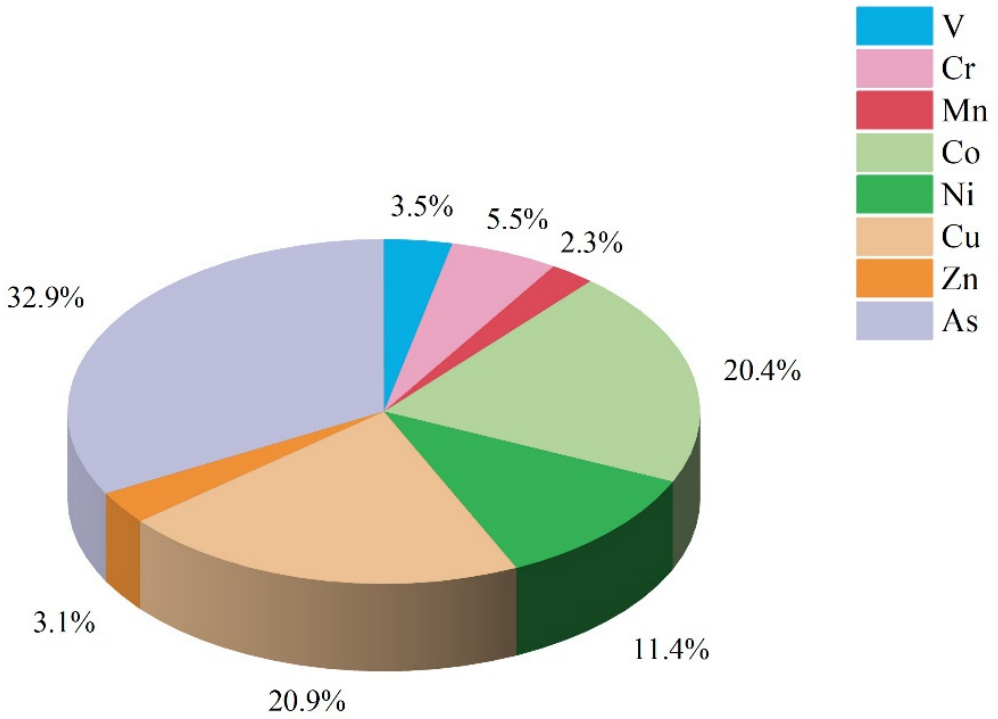

Figure 5. Contribution of eight heavy metals in dam sediment to E_r^i.

The degree of risk indicated by values of I_{geo} and E_r^i were generally similar. However, land accumulation index values indicated slight pollution, while E_r^i indicated high potential ecological risk. This difference results from the two methods having different emphases: I_{geo} provides an intuitive level of heavy metal pollution but doesn't discuss the harm of heavy metal pollution to organisms, while the E_r^i reflects the biological toxicity of heavy metals. The two metrics can be used in tandem to evaluate the risks associated with heavy metal pollution more comprehensively.

4. Discussion

4.1. Effects of Watershed Erosion and Sediment Yield on the Distribution of Heavy Metals

Check dam sediment can be used to restore soil in areas that have been degraded by heavy erosion [34]. The dam traps eroded materials from across the watershed, serving as a sink for sediment exported from the surrounding slopes [35]. Studies have shown that soil erosion is usually accompanied by the movement of pollutants. Due to the strong adsorption capacity of soil colloids, heavy metals are tightly bound to soil materials and migrate under the action of erosion [36]. Thus, eroded sediments may be enriched in any heavy metals contained within the watershed [36].

Human activities have significantly altered the properties of soil. Land use change (e.g., cultivation for use in agricultural production) results in compositional changes to local vegetation. The resulting difference in plant cover and root characteristics alters soil fertility, water retention, and other edaphic properties that influence microbial community structure. Collectively, these changes affect the behavior of heavy metals by altering patterns of pollutant migration and diffusion in the soil [37–39]. Before the 1990s, the Wangmaogou watershed was mainly sloping farmland. After the 1990s, conservationists successfully advocated for converting cropland to forest and grassland. Similar land use changes have been reported in the basin [38,40].

In this study (Figure 6), the total amount and deposition rates of heavy metals varied over time, with rates of heavy metal deposition peaking in 1963. Heavy rainfall coupled with severe erosion and sediment generation on slopes in the watershed resulted in the transport of large amounts of silt. As a result, heavy metals exhibited high rates of vertical migration, producing a spike in total heavy metal concentrations in dam sediments, with peaks in 1963, 1971, and 1986. These peaks correspond to historical heavy rainfall events (rainfall events of 1963/7 (55 mm), 1971/7 (87 mm), and 1986/8 (70 mm), in Figure 2), particularly in 1971 and 1986. Compared to trends in the subsequent periods (1968–1981, 1982, and 1985–1991), total heavy metal concentrations decreased gradually. This finding is consistent with other studies, linking the dam's location in a gully to the increased accumulation of easily transported materials (i.e., nutrients) from surrounding hillslopes. Moreover, higher rates of erosion are associated with an increase in phosphorus accumulation in dam water and sediment [40,41]. At the same time, the conversion from cultivated land to woodland or grassland promotes water infiltration into the soil, reduces sediment transport and runoff, and enhances soil organic carbon (SOC) storage [42,43]. Land use reversion to woodland or grassland results in SOC distribution [44]. In general, soil erosion and land use transitions are significant factors affecting soil nutrient and heavy metal contents.

4.2. Causes and Prevention Measures of Heavy Metal Pollution

Both the sources and effects of heavy metal pollution vary with land use [45,46]. In the surface soil of western Iran, for example, the content of heavy metals (Co and Ni) is related to the composition of the soil's parent material (a natural source) [47]. In contrast, Arsenic contamination in cultivated soils results from the extensive use of chemical fertilizers in agricultural production (an artificial source) [48]. In the area studied here, soil contamination assessment methods indicated a medium risk for Cu, Co, and As (Figure 7). The accumulation of these pollutants may be related to agricultural practices on land in the watershed's hillslope. For example, some fertilizers contain heavy metal elements, such as, Cr, Hg, and Ni, and some pesticide formulations (e.g., dicopper chloride trihydroxide, Bordeaux mixture) contain Cu and As [49]. In addition, manure applied as fertilizer has become an important source of heavy metals; these environmental contaminants are often added to livestock feed to prevent diseases and increase weight gain. Because heavy metals are poorly utilized by livestock, most of it is excreted in manure and urine. For example, cattle manure contains more than 90% of Cu consumed by the animal [50]. Thus, indiscriminate use of livestock manure by local farmers contributes to soil contamination. The history of land use in the basin and the results presented here suggest that the source of heavy metal pollution is largely caused by soil erosion and human activity. To minimize heavy

metal contamination in soils, the selection and dosage rates of nitrogen, phosphorus, and potassium fertilizers should be carefully managed. In addition, the migration of heavy metals can be attenuated by ensuring reasonable vegetation cover on hillslopes (i.e., reversion to grassland, shrubland, or forest). This practice can reduce soil erosion, intercept rainfall, and change surface runoff and hydrological processes. Moreover, beyond intercepting sediment and preventing river clogging, the check dam can control surrounding slope grades to mitigate soil erosion.

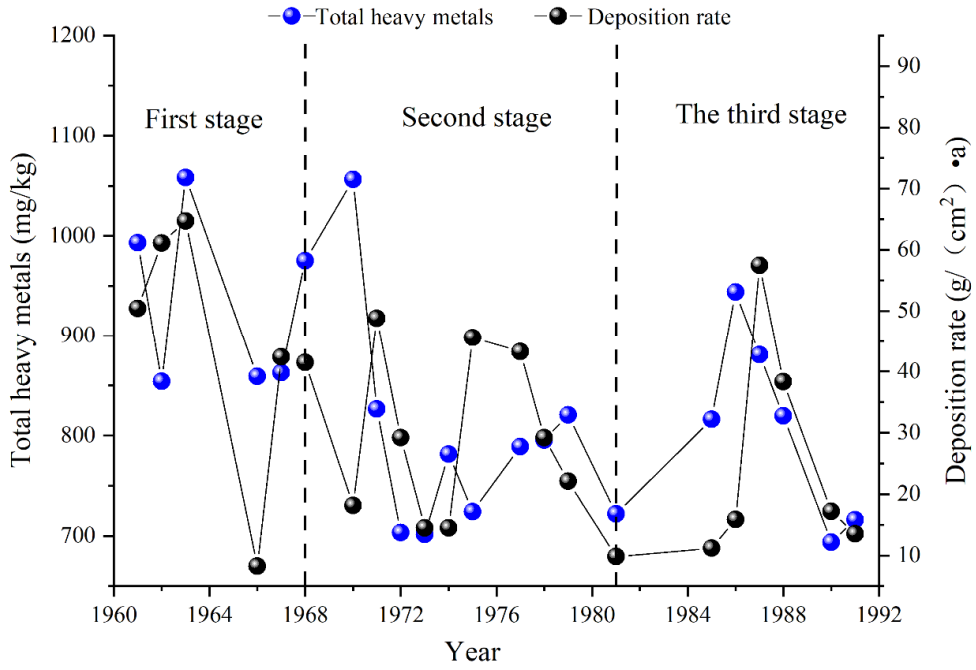

Figure 6. Variation of total amount and deposition rate of heavy metals over time.

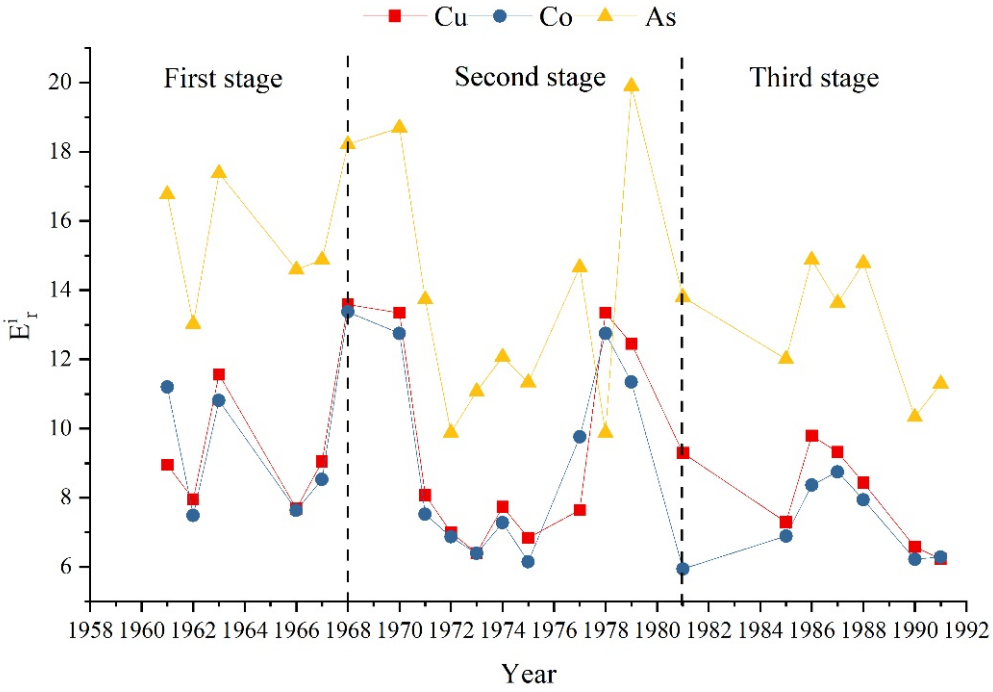

Figure 7. Variation of potential pollution index of heavy metals in sediments over time.

The deployment of multiple control measures can greatly reduce rates of erosion. Landscape degradation can be mitigated by adjusting the proportion of land used for

agriculture, forestry, and animal husbandry. When combined with judicious fertilization strategies, such as the application of passivators, soil conditioners, etc., the activity of pollutants in the soil could be reduced or eliminated. It is important to note that absorption of substances into soil materials converts toxic and harmful heavy metal ions from effective states into chemically inactive forms, thereby reducing their migration in the soil environment, their availability to plants, and their biological toxicity. By reducing rates of erosion and lowering contaminant inputs, risks to human health can be attenuated.

5. Conclusions

This investigation found that variations in the soil profile concentrations of eight heavy metals, considering depth and time, follow similar patterns. In the first (1960–1967) and second (1968–1981) periods investigated, the concentration of heavy metals greatly fluctuated. In the third period (1985–1991), the concentration of heavy metals tended to be stable. Erosion caused the longitudinal migration of heavy metals along the slope, resulting in the peak concentration of heavy metals in 1963, 1971, and 1986. Two soil pollution metrics indicated that the ecological risk of Cu pollution significantly increased in 1963, 1971, and 1986, which was closely related to the impact of land use decisions and slope water and soil loss. Agricultural production, particularly the indiscriminate use of chemical and organic fertilizers, is likely the main source of As and Cu contamination in dam sediments. Cu, Co, Mn, Ni, V, and Zn concentrations in the sediment reflect the composition of soil parent materials (i.e., natural sources). The potential ecological risks of As and Cu in the dam sediments are relatively high, indicating a need for additional mitigation efforts. Measures such as land use optimization and careful fertilizer use should be considered to reduce heavy metal pollution beyond the point sources.

Author Contributions: Conceptualization, Y.M. and P.L.; data curation, R.W.; formal analysis, Y.M. and L.X.; investigation, Y.M.; software, Y.M. and S.Y.; visualization, J.H. and B.H.; writing—original draft, Y.M.; writing—review and editing, Y.M., P.L. and L.X. All authors have read and agreed to the published version of the manuscript.

Funding: This study was financially supported by the National Natural Science Foundation of China (Grant No. 51779204 (Funder: Li, P.), Grant No. U2040208 (Funder: Li, Z.), Grant No. 42007070. (Funder: Zhao, B.)), Science and Technology Project of Clean Energy and Ecological Water Conservancy Engineering Research Center (Grant No. QNZX-2019-03 (Funder: Li, P.)), and Key Laboratory Project of Shaanxi Provincial Department of Education (Grant No. 20JS100 (Funder: Zhao, B.)).

Institutional Review Board Statement: Not applicable.

Informed Consent Statement: Not applicable.

Data Availability Statement: Not applicable.

Acknowledgments: We would like to thank Adam Roddy for assistance with the English language editing of this manuscript.

Conflicts of Interest: The authors declare no conflict of interest.

References

1. Ali, H.; Khan, E.; Ilahi, I. Environmental Chemistry and Ecotoxicology of Hazardous Heavy Metals: Environmental Persistence, Toxicity, and Bioaccumulation. *J. Chem.* **2019**, *2019*, 6730305. [CrossRef]
2. Yin, X.; Fan, G.; Liu, J.; Jiang, T.; Wang, L. Characteristics of heavy metals and persistent organic pollutants in PM2.5 in two typical industrial cities, North China. *Environ. Forensics* **2020**, *4*, 250–258. [CrossRef]
3. Bruland, K.W.; Bertine, K.; Koide, M.; Goldberg, E.D. History of metal pollution in southern california coastal zone. *Environ. Sci. Technol.* **1974**, *8*, 425–432. [CrossRef]
4. Lv, J.; Liu, Y.; Zhang, Z.; Dai, J.; Dai, B.; Zhu, Y. Identifying the origins and spatial distributions of heavy metals in soils of Ju country (Eastern China) using multivariate and geostatistical approach. *J. Soils Sediments* **2015**, *15*, 163–178. [CrossRef]
5. Miao, X.; Hao, Y.; Zhang, F.; Zou, S.; Ye, S.; Xie, Z. Spatial distribution of heavy metals and their potential sources in the soil of Yellow River Delta: A traditional oil field in China. Environ. *Geochem. Health* **2020**, *42*, 7–26. [CrossRef]

6. Liao, S.; Jin, G.; Khan, M.A.; Zhu, Y.; Duan, L.; Luo, W.; Jia, J.; Zhong, B.; Ma, J.; Ye, Z.; et al. The quantitative source apportionment of heavy metals in peri-urban agricultural soils with UNMIX and input fluxes analysis. *Environ. Technol. Innov.* **2021**, *21*, 101232. [CrossRef]
7. Du, C.; Wu, J.; Bashir, M.H.; Shaukat, M.; Ali, S. Heavy metals transported through a multi-trophic food chain influence the energy metabolism and immune responses of Cryptolaemus montrouzieri. *Ecotoxicology* **2019**, *28*, 422–428. [CrossRef]
8. Uchimiya, M.; Wartelle, L.H.; Klasson, K.T.; Fortier, C.A.; Lima, I.M. Influence of Pyrolysis Temperature on Biochar Property and Function as a Heavy Metal Sorbent in Soil. *J. Agric. Food Chem.* **2011**, *59*, 2501–2510. [CrossRef]
9. Cipullo, S.; Snapir, B.; Tardif, S.; Campo, P.; Prpich, G.; Coulon, F. Insights into mixed contaminants interactions and its implication for heavy metals and metalloids mobility, bioavailability and risk assessment. *Sci. Total Environ.* **2018**, *645*, 662–673. [CrossRef]
10. Han, X.; Xiao, J.; Wang, L.; Tian, S.; Liang, T.; Liu, Y. Identification of areas vulnerable to soil erosion and risk assessment of phosphorus transport in a typical watershed in the Loess Plateau. *Sci. Total Environ.* **2021**, *758*, 143661. [CrossRef]
11. Zhang, J.; Yang, M.; Zhang, F.; Tang, Y.; Wang, X.; Wang, Y. Revealing soil erosion characteristics using deposited sediment sources in a complex small catchment in the wind-water erosion crisscross region of the Chinese Loess Plateau. *Geoderma* **2020**, *379*, 114634. [CrossRef]
12. Guo, M.; Chen, Z.; Wang, W.; Wang, T.; Wang, W.; Cui, Z. Revegetation induced change in soil erodibility as influenced by slope situation on the Loess Plateau. *Sci. Total Environ.* **2021**, *772*, 145540. [CrossRef] [PubMed]
13. Wu, L.; Liu, X.; Ma, X. Spatio-temporal variation of erosion-type non-point source pollution in a small watershed of hilly and gully region, Chinese Loess Plateau. *Environ. Sci. Pollut. R* **2016**, *23*, 10957–10967. [CrossRef]
14. Zhao, Q.; Bai, J.; Gao, Y.; Zhang, G.; Lu, Q.; Jia, J. Heavy metal contamination in soils from freshwater wetlands to salt marshes in the Yellow River Estuary, China. *Sci. Total Environ.* **2021**, *774*, 145072. [CrossRef]
15. Tóth, G.; Hermann, T.; Da Silva, M.R.; Montanarella, L. Heavy metals in agricultural soils of the European Union with implications for food safety. *Environ. Int.* **2016**, *88*, 299–309. [CrossRef]
16. Sun, C.; Zhu, S.; Zhao, B.; Li, W.; Gao, X.; Wang, X. Effect of Land Use Conversion on Surface Soil Heavy Metal Contamination in a Typical Karst Plateau Lakeshore Wetland of Southwest China. *Int. J. Environ. Res. Public Health* **2020**, *17*, 84. [CrossRef]
17. Rao, Q.; Sun, Z.; Tian, L.; Li, J.; Sun, W.; Sun, W. Assessment of arsenic and heavy metal pollution and ecological risk in inshore sediments of the Yellow River estuary, China. *Stoch. Environ. Res. Risk Assess.* **2018**, *32*, 2889–2902. [CrossRef]
18. Sarker, K.K.; Bristy, M.S.; Alam, N.; Baki, M.A.; Shojib, F.H.; Quraishi, S.B.; Khan, M.F. Ecological risk and source apportionment of heavy metals in surface water and sediments on Saint Martin's Island in the Bay of Bengal. *Environ. Sci. Pollut. Res.* **2020**, *27*, 31827–31840. [CrossRef]
19. Singh, B.P.; Choudhury, M.; Samanta, P.; Gaur, M.; Kumar, M. Ecological Risk Assessment of Heavy Metals in Adjoining Sediment of River Ecosystem. *Sustainability* **2021**, *13*, 10330. [CrossRef]
20. Liao, J.; Chen, J.; Ru, X.; Chen, J.; Wu, H.; Wei, C. Heavy metals in river surface sediments affected with multiple pollution sources, South China: Distribution, enrichment and source apportionment. *J. Geochem. Explor.* **2017**, *176*, 9–19. [CrossRef]
21. Zhang, Z.; Lu, Y.; Li, H.; Tu, Y.; Liu, B.; Yang, Z. Assessment of heavy metal contamination, distribution and source identification in the sediments from the Zijiang River, China. *Sci. Total Environ.* **2018**, *645*, 235–243. [CrossRef]
22. Debnath, A.; Singh, P.K.; Chandra, S.Y. Metallic contamination of global river sediments and latest developments for their remediation. *J. Environ. Manag.* **2021**, *298*, 113378. [CrossRef] [PubMed]
23. Zhang, Y.; Zhang, X.; Bi, Z.; Yu, Y.; Shi, P.; Ren, L.; Shan, Z. The impact of land use changes and erosion process on heavy metal distribution in the hilly area of the Loess Plateau, China. *Sci. Total Environ.* **2020**, *718*, 137305. [CrossRef]
24. Chen, L.; Wu, J.; Xia, C.; Gong, L.; Xu, Z. Chemical speciation and potential ecological risk assessment of heavy metals in volcanic rocks of Southern Qinghai, China. *Chem. Ecol.* **2019**, *35*, 775–787. [CrossRef]
25. Chen, Z.; Huang, S.; Chen, L.; Cheng, B.; Li, M.; Huang, H. Distribution, source, and ecological risk assessment of potentially toxic elements in surface sediments from Qingfeng River, Hunan, China. *J. Soil Sediments* **2021**, *21*, 2686–2698. [CrossRef]
26. You, M.; Hu, Y.; Yan, Y.; Yao, J. Speciation Characteristics and Ecological Risk Assessment of Heavy Metals in Municipal Sludge of Huainan, China. *Molecules* **2021**, *26*, 6711. [CrossRef]
27. Custodio, M.; Fow, A.; Chanamé, F.; Orellana-Mendoza, E.; Peñaloza, R.; Alvarado, J.C.; Cano, D.; Pizarro, S. Ecological Risk Due to Heavy Metal Contamination in Sediment and Water of Natural Wetlands with Tourist Influence in the Central Region of Peru. *Water* **2021**, *13*, 2256. [CrossRef]
28. Kang, D.; Zheng, G.; Yu, J.; Chen, Q.; Zheng, X.; Zhong, J.; Zhang, Y.; Ding, H.; Zhang, Y. Hydropower reservoirs enhanced the accumulation of heavy metals towards surface sediments and aggravated ecological risks in Jiulong River Basin, China. *J. Soil Sediments* **2021**, *21*, 3479–3492. [CrossRef]
29. Hakanson, L. An ecological risk index for aquatic pollution control.a sedimentological approach. *Water Res.* **1980**, *14*, 975–1001.
30. Xu, Z.Q.; Ni, S.J.; Tuo, X.G.; Zhang, C.J. Calculation of heavy metal's toxicity coefficient in the evaluation of potential ecological risk index. *Environ. Sci. Technol.* **2008**, *31*, 112–115. (In Chinese)
31. Li, M.; YongXin, N.; XiZhi, L.; QiuFen, Z.; Nan, L.L. Study on sedimentary characteristics of warping dam under different silting states in Chabagou watershed. *IOP Conf. Ser. Earth Environ. Sci.* **2021**, *687*, 12034. [CrossRef]
32. Jaakkola, T.; Tolonen, K.; Huttunen, P.; Leskinen, S. The use of fallout ^{137}Cs and 239,240Pu for dating of lake sediments. *Hydrobiologia* **1983**, *103*, 15–19. [CrossRef]

33. Ivanov, M.M.; Konoplev, A.V.; Walling, D.E.; Konstantinov, E.A.; Gurinov, A.L.; Ivanova, N.N.; Kuzmenkova, N.V.; Tsyplenkov, A.S.; Ivanov, M.A.; Golosov, V.N. Using reservoir sediment deposits to determine the longer-term fate of chernobyl-derived ^{137}Cs fallout in the fluvial system. *Environ. Pollut.* **2021**, *274*, 116588. [CrossRef]
34. Wang, Y.; Chen, L.; Fu, B.; Lü, Y. Check dam sediments: An important indicator of the effects of environmental changes on soil erosion in the Loess Plateau in China. Environ. *Monit. Assess.* **2014**, *186*, 4275–4287. [CrossRef]
35. Yu, Q.; Nagataki, S.; Lin, J.; Saeki, T.; Hisada, M. The leachability of heavy metals in hardened fly ash cement and cement-solidified fly ash. *Cem. Concr. Res.* **2005**, *35*, 1056–1063. [CrossRef]
36. Quinton, J.N.; Catt, J.A. Enrichment of heavy metals in sediment resulting from soil erosion on agricultural fields. *Environ. Sci. Technol.* **2007**, *41*, 3495–3500. [CrossRef]
37. Tepanosyan, G.; Sahakyan, L.; Belyaeva, O.; Asmaryan, S.; Saghatelyan, A. Continuous impact of mining activities on soil heavy metals levels and human health. *Sci. Total Environ.* **2018**, *639*, 900–909. [CrossRef]
38. Wu, Y.; Yang, L.; Büyüksönmez, F.; Beighley, R.E.; Gu, Z.; Grey, M. Evaluation of Soil Erosion and Sediment Control Products for Release of Heavy Metals. *Environ. Eng. Sci.* **2010**, *27*, 905–914. [CrossRef]
39. Yan, X.; Liu, M.; Zhong, J.; Guo, J.; Wu, W. How Human Activities Affect Heavy Metal Contamination of Soil and Sediment in a Long-Term Reclaimed Area of the Liaohe River Delta, North China. *Sustainability* **2018**, *10*, 338. [CrossRef]
40. Long, Z.; Huang, Y.; Zhang, W.; Shi, Z.; Yu, D.; Chen, Y.; Liu, C.; Wang, R. Effect of different industrial activities on soil heavy metal pollution, ecological risk, and health risk. *Environ. Monit. Assess.* **2021**, *193*, 20. [CrossRef]
41. Zhang, Y.; Li, P.; Liu, X.; Xiao, L.; Shi, P.; Zhao, B. Effects of farmland conversion on the stoichiometry of carbon, nitrogen, and phosphorus in soil aggregates on the Loess Plateau of China. *Geoderma* **2019**, *351*, 188–196. [CrossRef]
42. Cheng, Y.; Li, P.; Xu, G.; Li, Z.; Gao, H.; Zhao, B.; Wang, T.; Wang, F.; Cheng, S. Effects of soil erosion and land use on spatial distribution of soil total phosphorus in a small watershed on the Loess Plateau, China. *Soil Tillage Res.* **2018**, *184*, 142–152. [CrossRef]
43. Zhang, Y.; Li, P.; Liu, X.; Xiao, L.; Li, Z.; Wu, H.; Zhou, S.; Ren, M. Tracer elements revealed the soil organic carbon sources in a dam-controlled watershed. *Soil Tillage Res.* **2022**, *216*, 105184. [CrossRef]
44. Li, Z.; Liu, C.; Dong, Y.; Chang, X.; Nie, X.; Liu, L.; Xiao, H.; Lu, Y.; Zeng, G. Response of soil organic carbon and nitrogen stocks to soil erosion and land use types in the Loess hilly–gully region of China. *Soil Tillage Res.* **2017**, *166*, 1–9. [CrossRef]
45. Huang, J.; Guo, S.; Zeng, G.; Li, F.; Gu, Y.; Shi, Y.; Shi, L.; Liu, W.; Peng, S. A new exploration of health risk assessment quantification from sources of soil heavy metals under different land use. *Environ. Pollut.* **2018**, *243*, 49–58. [CrossRef]
46. Lu, Q.; Wang, S.; Bai, X.; Liu, F.; Li, C.; Deng, Y.; Tian, S. Quantitative assessment of human health risks under different land uses based on soil heavy metal pollution sources. *Hum. Ecol. Risk Assess.* **2020**, *27*, 327–343. [CrossRef]
47. El-Naggar, A.; Shaheen, S.M.; Ok, Y.S.; Rinklebe, J. Biochar affects the dissolved and colloidal concentrations of Cd, Cu, Ni, and Zn and their phytoavailability and potential mobility in a mining soil under dynamic redox-conditions. *Sci. Total Environ.* **2018**, *624*, 1059–1071. [CrossRef]
48. Taghipour, M.; Ayoubi, S.; Khademi, H. Contribution of Lithologic and Anthropogenic Factors to Surface Soil Heavy Metals in Western Iran Using Multivariate Geostatistical Analyses. *Soil Sediment Contam.* **2011**, *20*, 921–937. [CrossRef]
49. Ahmed, A.; Sara Taha, A.; Sundas, R.Q.; Man-Qun, W. Plants: Ecological Risks and Human Health Implications. *Toxics* **2021**, *9*, 42.
50. Provolo, G.; Manuli, G.; Finzi, A.; Lucchini, G.; Riva, E.; Sacchi, G. Effect of Pig and Cattle Slurry Application on Heavy Metal Composition of Maize Grown on Different Soils. *Sustainability* **2018**, *10*, 2684. [CrossRef]